ChemComm

RSCPublishing

COMMUNICATION

View Article Online
View Journal

Cite this: DOI: 10.1039/c3cc45011b

Received 4th July 2013,
Accepted 8th August 2013

DOI: 10.1039/c3cc45011b

www.rsc.org/chemcomm

# Laminated nanotapes fabricated from conformation specific self-assembly of *N*-annulated perylene derivatives†

Kai Sun, Yan Li* and Wenxin Fu*

**Laminated nanotapes were fabricated *via* conformation specific self-assembly of two *N*-annulated perylene derivatives (NPDs). The assemblies in solvated states were characterized using cryogenic transmission electron microscopy (cryo-TEM), and their nanostructures were modulated by the synergistic interactions of π–π stacking and hydrogen bonds.**

Highly ordered one dimensional supramolecular structures such as nanowires and nanotapes formed from organic semiconductor molecules have attracted considerable research interests due to their potential in optoelectronic devices.[1] Constructing well-defined nanostructures from functionalized graphene was believed to be a strategy with great potential.[2] Various nanostructures such as nanowires,[3] nanobelts,[4] nanosheets,[5] and nanotubes[6] have been constructed from self-assembly of aromatic organic molecules.[7] Researchers could make full use of multiple intermolecular interactions, such as π–π stacking, hydrogen bonds, hydrophilic–hydrophobic interactions, van der Waals force, *etc.*, to tune and optimize the assembled nanostructures.[8] In addition, the substructure of building blocks and assembly conditions (solvent polarity and concentration) were demonstrated to have profound effects on the resultant morphology as well.[9]

Recently, we reported a new efficient synthetic method to prepare solvent processable bis-*N*-annulated quaterrylenes (BNQs) and tri-*N*-annulated hexarylenes (TNHs) from easily available *N*-annulated perylene derivatives. BNQs and TNHs exhibited strong fluorescence, large dipole moments and liquid crystalline properties.[10] Here, we report the formation of laminated nanotapes from two NPDs, from which sub-millimeter long one-dimensional structures were obtained under optimized conditions. The nanostructures of assemblies can be modulated by synergistic interactions of π–π stacking and hydrogen bonds. Moreover, we found that a slight variation of the molecular conformation can switch the orientation of building molecules within nanotapes. Note that the cryo-TEM technique allowed direct imaging of solvated supramolecular assemblies and avoided artifacts to a great extent.

Scheme 1 shows the chemical structures and preferred conformation of two NPDs, which were synthesized according to the procedure given in the literature[11] (see Scheme S1 in the ESI†). The only difference between **1** and **2** was that **2** had fused perylene rings to give a completely planar conjugated molecule, while the perylene rings of **1** had a twisted angle to lower their free energy. Such rotation will give rise to rotational entropy for **1**,[12] which thus had much better solubility in common organic solvents than **2**.[13] Both **1** and **2** can be easily dispersed in polar solvents, such as THF, DMF, *etc.*, but are insoluble in nonpolar solvents, such as hexane and toluene. Solution self-assemblies of **1** and **2** were induced *via* direct dissolution of solid compounds into THF. Cryo-TEM measurements revealed that both **1** and **2** formed nanotapes with width between 50 and 200 nm and length ranging from 100 to 1000 nm (Fig. 1). More cryo-TEM images of the assemblies are shown in Fig. S1 (see ESI†).

Then, we investigated the effects of concentration on self-assembly behaviors using UV/Vis absorption (Fig. 2) and fluorescence spectra (see Fig. S3 in the ESI†). From the absorption spectra, the main absorption peaks of both **1** and **2** did not move with the increase of concentration, indicating insignificant change of their own coupling excitons,[14] which were further confirmed by

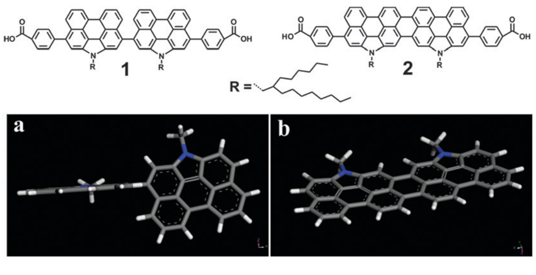

**Scheme 1** Chemical structures of **1** and **2** (Top). Optimized conformation of the two perylene rings by Gaussian 03 for **1** (a) and **2** (b), respectively.

---

*Beijing National Laboratory for Molecular Sciences, Institute of Chemistry, Chinese Academy of Sciences, Beijing 100190, P. R. China. E-mail: fuwenxin@iccas.ac.cn, yanli@iccas.ac.cn*

† Electronic supplementary information (ESI) available: Details of synthesis, additional SEM images, cryo-TEM images, XRD patterns and SAED images. See DOI: 10.1039/c3cc45011b

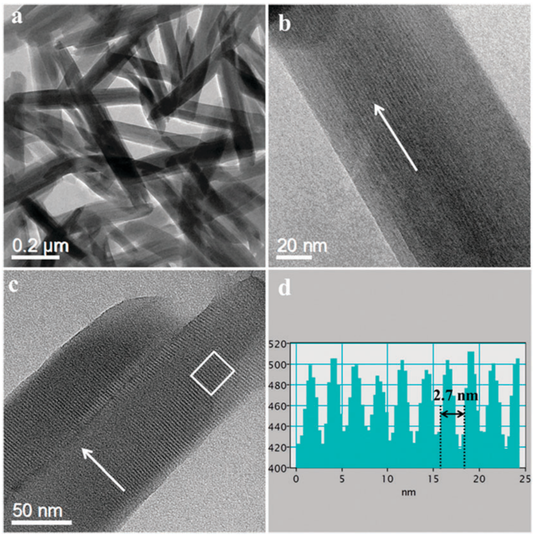

**Fig. 1** Cryo-TEM images of assemblies formed from **1** (a, b) and **2** (c) in 1 mM THF and the corresponding spacing profile (d) of white rectangle in (c). The white arrows in (b) and (c) represent the direction of hydrogen bonds between NPD monomers.

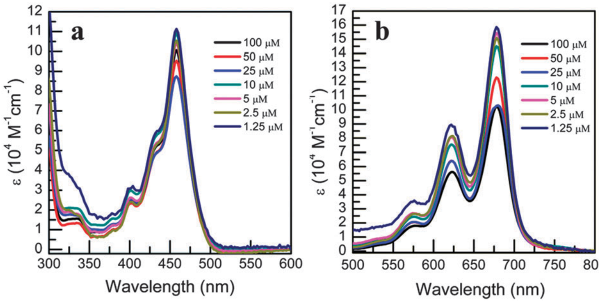

**Fig. 2** UV/Vis absorption spectra of **1** (a) and **2** (b) in THF at different concentrations.

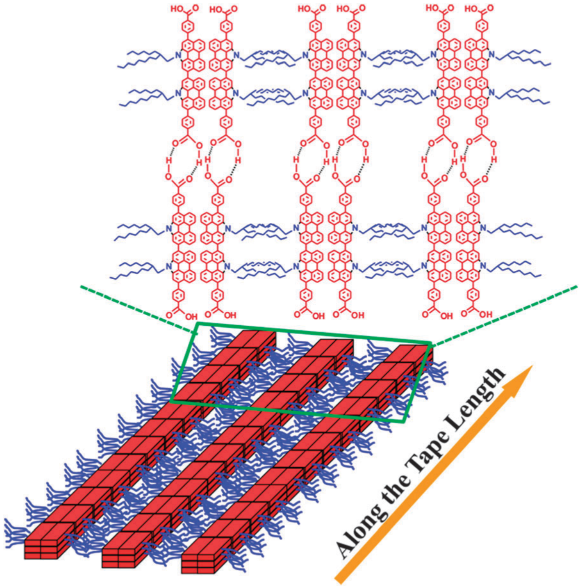

**Scheme 2** Schematic illustration of the self-assembly mechanism for **1** with the head-to-head and tail-to-tail models. In order to compare to **2** (in Scheme S2, ESI†), we simplify the twisted perylene rings of **1** as a plane.

cryo-TEM measurements at low concentrations (see Fig. S2 in the ESI†). It was also interesting to emphasize that both **1** and **2** had large absorption coefficients and formed aggregates even at $10^{-6}$ M THF, indicating that they had strong intermolecular interactions (π–π stacking, hydrogen bonds and dipole–dipole interactions), which agreed well with the previous results.[10] In contrast, the fluorescence spectra of **2** displayed a slightly bathochromic shift with the increase of concentration from 1.25 to 100 μM, probably due to the inner filter effects (reabsorption).

Interestingly, careful examination using high resolution transmission electron microscopy (HRTEM) revealed that both **1** and **2** actually formed lamellar nanostructures (Fig. 1b and c). As the samples were still in solvated states, we attributed the dark region to the planar aromatic ring domains and the grey region to alkyl side chain domains considering their electron density differences. TEM and FFT transfer showed that the dark region was about 1.2 nm wide and the grey region was about 1.5 nm wide. It is well-known that the distance of π–π stacking is about 0.35 nm, we thus assumed that laminated structures had to adopt a distinct packing motif.

Considering the molecular dimensions of **1** and **2**, we proposed a head-to-head and tail-to-tail packing model for their resulting nanotapes illustrated in Scheme 2 and Scheme S2 (see ESI†). From the molecular structure, the width of the perylene ring is about 0.5 nm, so two head-to-head packing perylenes will give a width of ∼1 nm as the J-type aggregation.[15] In addition, the length of fully extended C-10 alkyl side chains is around 1.2 nm provided that they adopt the zig-zag conformation. Partially interdigitation of two alkyl chains can result in a dimension of 1.5 nm, which had great consistency with the cryo-TEM results (Fig. 1). Based on the above information, we proposed that the perylene rings adopted a face-up orientation as illustrated in Scheme 2.

Also note that the two NPDs have different orientations within flat nanotapes, namely along and perpendicular to the long axis of perylene rings for **1** and **2**, respectively. We believed that it was induced by different growth kinetics. Firstly, both **1** and **2** preferred stacking perpendicular to the flat tape *via* π–π interactions, which were supported by XRD characterizations (see Fig. S4 in ESI†). Secondly, sample **2** with flat conformation might need less energy to arrange a head-to-head packing in polar solvent medium. In contrast, sample **1** will have extra entropy penalty arising from the rotational freedom between two perylene rings that prefer having twisted arrangements. As a result, growing along carboxylic acid will be preferred for **1**. In contrast, the nanotape's growth direction was perpendicular to the hydrogen bonds for **2**.

More importantly, the hydrogen bonds were also critical for forming laminated nanotapes. We prepared samples **1′** and **2′**, which had similar structures to **1** and **2** except that **1′** and **2′** contained two ester bonds instead of carboxylic acid. Surprisingly, both **1′** and **2′** only formed amorphous structures regardless of self-assembly conditions (see Fig. S5 in ESI†).

Considering that long range ordering is desirable for nanodevices, we attempted to employ a selective solvent to promote the growth of preformed nanotapes. Toluene (a poor solvent for the two NPDs) was added to sample THF solutions to induce

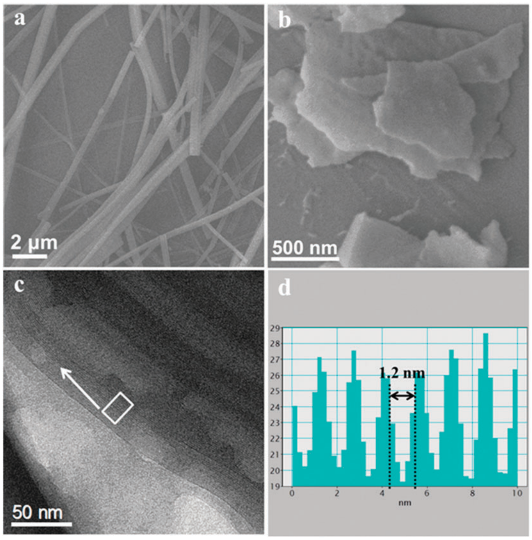

**Fig. 3** SEM (a, b) and cryo-TEM (c) images of supramolecular assemblies formed from the two NPDs: (a, c) **1** in THF–toluene (1/19, v/v) mixed solvents ($C$ = 0.05 mM); (b) **2** in THF–toluene (1/9, v/v) mixed solvents ($C$ = 0.01 mM); (d) the corresponding spacing profile of a white rectangle in (c). The white arrow in (c) represents the direction of hydrogen bonds between NPD monomers. The SEM sample was prepared by drop-casting the assembly suspension on a silicon wafer.

their crystallization. For sample **2** in 0.01 mM THF–toluene (1/9, v/v), a macroscopic phase separation occurred after a few hours. The precipitates were found to be irregular plates (Fig. 3b). In contrast, dilution of 0.1 mM THF solution of **1** with 9-fold toluene did not induce phase separation after one week. However, as the concentration rose to 0.05 mM in THF–toluene (1/19, v/v), needle-like crystals started to appear after 24 hours quiescence and became larger and larger with time. These aggregations were found to be tens of micrometers long nanotapes, which were composed of layered nanotapes (Fig. 3a). More SEM and TEM images with different magnifications are shown in Fig. S7 and S8 (see ESI†). The width of each layer was between 200 nm and 1 μm, and the thickness of each nanotape was around 50 nm. HRTEM examination (Fig. 3c and d) revealed that these nanotapes had lamellar morphology with the dark regions of ~1.2 nm, which were identical to those formed in THF (Fig. 1d). However, the grey region was shrunk to 0.6 nm. The reason was probably due to collapse of the flexible alkyl group. The selected area electron diffraction (SAED) pattern of the needle-like crystals in Fig. S9 (see ESI†) confirm ordered arrangements within the crystals.

Given the results discussed above, we believed that the interaction between the molecule and the solvent was the key to the formation of highly ordered supramolecular structures. Generally, toluene was a poor solvent for both solid compounds. But for the flat **2** dissolved in THF, the π–π interaction between toluene and the compound was enhanced,[16] which even could disassemble the preformed nanotapes to a certain extent. With more toluene, a macroscopic phase separation occurred. So with the increase of toluene, the system went through two stages, from disassembly to amorphous aggregates. In contrast, for twisted perylene rings **1**, the π–π interaction between toluene and **1** was not strong enough to break that among molecules. Hence, as a poor solvent, toluene just induced the preformed nanotapes to further reassemble larger ones.

In summary, we have demonstrated that two *N*-annulated perylene derivatives with different conformations have different self-assembly behaviors. Molecular self-assembly revealed that they have different abilities to form large nanotapes with variable sizes under different conditions, which provides an insight into control and optimization of molecular parameters and solvent effects to tune resulting morphologies.

This work was supported by National Natural Science Foundation of China (51225306, 91027043 and 21204091). We thank Prof. Zhibo Li and Prof. Zhaohui Wang for their advice on synthesis and characterization.

## Notes and references

1 L. Zang, Y. Che and J. S. Moore, *Acc. Chem. Res.*, 2008, **41**, 1596; F. Würthner, *Chem. Commun.*, 2004, 1564; A. C. Grimsdale and K. Müllen, *Angew. Chem., Int. Ed.*, 2005, **44**, 5592; F. Würthner and M. Stolte, *Chem. Commun.*, 2011, **47**, 5109.

2 V. Palermo, *Chem. Commun.*, 2013, **49**, 2848; J. Wu, W. Pisula and K. Müllen, *Chem. Rev.*, 2007, **107**, 718; V. Georgakilas, M. Otyepka, A. B. Bourlinos, V. Chandra, N. Kim, K. C. Kemp, P. Hobza, R. Zboril and K. S. Kim, *Chem. Rev.*, 2012, **112**, 6156.

3 A. Datar, D. E. Gross, K. Balakrishnan, X. Yang, J. S. Moore and L. Zang, *Chem. Commun.*, 2012, **48**, 8904.

4 A. Lv, S. R. Puniredd, J. Zhang, Z. Li, H. Zhu, W. Jiang, H. Dong, Y. He, L. Jiang, Y. Li, W. Pisula, Q. Meng, W. Hu and Z. Wang, *Adv. Mater.*, 2012, **24**, 2626; K. Balakrishnan, A. Datar, R. Oitker, H. Chen, J. Zuo and L. Zang, *J. Am. Chem. Soc.*, 2005, **127**, 10496.

5 J. A. Lehrman, H. Cui, W.-W. Tsai, T. J. Moyer and S. I. Stupp, *Chem. Commun.*, 2012, **48**, 9711.

6 J. P. Hill, W. Jin, A. Kosaka, T. Fukushima, H. Ichihara, T. Shimomura, K. Ito, T. Hashizume, N. Ishii and T. Aida, *Science*, 2004, **304**, 1481.

7 F. J. M. Hoeben, P. Jonkheijm, E. W. Meijer and A. P. H. J. Schenning, *Chem. Rev.*, 2005, **105**, 1491.

8 A. D'Urso, M. E. Fragala and R. Purrello, *Chem. Commun.*, 2012, **48**, 8165; Y. F. Zhou and D. Y. Yan, *Chem. Commun.*, 2009, 1172.

9 Y. Sun, C. He, K. Sun, Y. Li, H. Dong, Z. Wang and Z. Li, *Langmuir*, 2011, **27**, 11364; D. Roy, J. N. Cambre and B. S. Sumerlin, *Chem. Commun.*, 2009, 2106; R. Nagarajan and E. Ruckenstein, *Langmuir*, 1991, 7, 2934.

10 Y. Li and Z. Wang, *Org. Lett.*, 2009, **11**, 1385; Y. Li, L. Hao, H. Fu, W. Pisula, X. Feng and Z. Wang, *Chem. Commun.*, 2011, **47**, 10088; Y. Li, J. Gao, S. Di Motta, F. Negri and Z. Wang, *J. Am. Chem. Soc.*, 2010, **132**, 4208.

11 A. Tsuda and A. Osuka, *Science*, 2001, **293**, 79; S. Hiroto and A. Osuka, *J. Org. Chem.*, 2005, **70**, 4054; A. Tsuda, H. Furuta and A. Osuka, *Angew. Chem., Int. Ed.*, 2000, **39**, 2549.

12 K. L. Mardis, *J. Phys. Chem. B*, 2005, **110**, 971; M. S. Searle and D. H. Williams, *J. Am. Chem. Soc.*, 1992, **114**, 10690; E. Darian, V. Hnizdo, A. Fedorowicz, H. Singh and E. Demchuk, *J. Comput. Chem.*, 2005, **26**, 651.

13 S. H. Yalkowsky, *Ind. Eng. Chem. Fundam.*, 1979, **18**, 108; A. F. M. Barton, *Chem. Rev.*, 1975, **75**, 731; G. N. Patel, R. R. Chance and J. D. Witt, *J. Chem. Phys.*, 1979, **70**, 4387.

14 J. K. Gallaher, E. J. Aitken, R. A. Keyzers and J. M. Hodgkiss, *Chem. Commun.*, 2012, **48**, 7961; T. Heek, C. Fasting, C. Rest, X. Zhang, F. Würthner and R. Haag, *Chem. Commun.*, 2010, **46**, 1884.

15 F. Würthner, T. E. Kaiser and C. R. Saha-Möller, *Angew. Chem., Int. Ed.*, 2011, **50**, 3376.

16 C. A. Hunter and J. K. M. Sanders, *J. Am. Chem. Soc.*, 1990, **112**, 5525.